

Spatiotemporal environmental triggers of Ebola and Marburg virus transmission

R. Ryan Lash^a, Nathaniel A. Brunsell^a and A. Townsend Peterson^{b*}

^aDepartment of Geography, The University of Kansas, Lawrence, Kansas, USA; ^bThe Natural History Museum and Biodiversity Research Center, The University of Kansas, Lawrence, Kansas, USA

(Received 19 March 2007; final version received 1 May 2008)

Despite their fame, Ebola and Marburg viruses (family *Filoviridae*) remain mysterious. Filovirus outbreaks are restricted to tropical Africa, but their likely geographic extent has been outlined only recently, and their natural reservoir host(s) remains unidentified. If environmental conditions associated with outbreaks in space and time can be identified precisely, much could be learned about the ecology, evolution and transmission of these viruses. We examined five filovirus outbreaks for which time series of remotely sensed data (NDVI values) are available and for which the reservoir-to-human index case transmission timing and location are known. A wavelet analysis was used to detect anomalous behaviour in the NDVI signal across multiple time scales for each outbreak. Scale-wise anomalies were manifested at a 20-day scale, and were found in four of the five sites, one to three weeks preceding outbreaks, suggesting that filovirus-caused disease outbreaks may be associated with either behavioural shifts in a vertebrate host or changes in viral population dynamics. More generally, wavelet analysis offers a powerful tool for identifying temporal correlates of disease transmission events.

Keywords: Ebola virus; disease ecology; NDVI; wavelet analysis; temporal analysis

1. Introduction

Remotely sensed (RS) data have been used to study temporal and spatial correlates in several disease systems (Beck *et al.* 2000, Hay *et al.* 1997). Connections between RS data and disease outbreaks have been generalized as a two-part process: (1) RS data provide information about weather, land cover and vegetation phenology; (2) weather, land cover and phenology in turn affect aspects of disease reservoir or vector distribution and behaviour (Mills and Childs 1998, Curran *et al.* 2000). When spatiotemporal characteristics of the processes linking the various parts of the disease transmission system are understood, cryptic causal factors may become more apparent (Glass *et al.* 2000, Yates *et al.* 2002).

1.1 *Filovirus disease ecology*

The viral family *Filoviridae* is composed of two genera, *Ebolavirus* and *Marburgvirus* (Murphy *et al.* 1978). For all their fame, however, filoviruses have only been known for

*Corresponding author. Email: town@ku.edu

17 years, with Marburg appearing in an imported outbreak in Germany and Yugoslavia in 1967, and Ebola appearing in simultaneous (but unconnected) outbreaks in the Democratic Republic of the Congo and Sudan in 1976 (World Health Organization 1978a,b). In spite of intensive research on many fronts, the details of ecology, etiology, and natural history of the filoviruses have remained opaque to essentially all inquiry. Of what is known of filovirus ecology, the first details came from epidemiological investigations of outbreak sites (Conrad *et al.* 1978, Breman *et al.* 1999, Georges *et al.* 1999, Leirs *et al.* 1999, Bausch *et al.* 2003). Although a recent study purported to have identified the sylvatic reservoir of these viruses (Leroy *et al.*, 2005), uncertainties remain regarding their results (see Section 4). Several studies have now approached issues of filovirus ecology quantitatively (Tucker *et al.* 2002, Peterson *et al.* 2004a,b, Pinzon *et al.* 2004, Walsh *et al.* 2005), but only partial lessons have been learned: Ebola is a phenomenon of humid rainforest, while Marburg occurs in drier and more seasonal forests; and some suggestion exists of consistent climatic signals leading up to Ebola outbreaks. More generally, it is clear that filoviruses are an animal disease, or zoonosis (Leroy *et al.* 2005) likely held in a mammal reservoir (Peterson *et al.* 2004b). Although other mammalian zoonoses are known to respond to environmental signals (Glass *et al.* 2000), filovirus transmission is rare, and may represent either very unusual environmental circumstances or more common conditions coupled with significant random elements. As such, this study is designed to ask whether consistent environmental signals can be discerned among the temporal variation in conditions at outbreak sites.

1.2 RS data

Links between RS data and complex landscape and vegetation phenomena and processes have been documented amply. The advanced very high resolution radiometer (AVHRR) sensor was launched aboard the National Oceanic and Atmospheric Administration (NOAA) polar orbiting satellite in 1978 (Cracknell 1997) to collect five bands of radiometric data at a spatial resolution of ~ 1.1 km, with daily coverage of the entire planet. Tucker (1979) identified a ratio between the red and near-infrared bands as most strongly correlated to photosynthetic material, and band ratioing has also been found to be useful in correcting topographically induced error (Holben and Justice 1981). This index, the normalized difference vegetation index (NDVI), also accounts for variation in the solar zenith angle (Townshend and Tucker 1984), and is calculated based on surface reflectance in the near-infrared and red bands.

In tropical equatorial regions, passive RS systems are hampered by cloud cover, and all systems have geometric inaccuracies induced by off-nadir viewing (i.e. when data are collected at angles not perpendicular to the Earth's surface). To minimize both of these effects, a temporal compositing technique was developed, in which the highest daily NDVI value from several daily images (Holben 1986) is selected, enabling long-term vegetation studies to be comparable over large areas. With global coverage of NDVI data as a highest priority (James and Kalluri 1994), the Pathfinder programme facilitated continental and global research (Maiden and Greco 1994), in part by making available 10-day maximum NDVI composite images with a global extent, excluding polar regions.

Temporal AVHRR NDVI composites have been used to monitor vegetation patterns across all of Africa (Townshend and Justice 1986), as well as vegetation and rainfall patterns in eastern Africa (Justice *et al.* 1986). Henricksen and Durkin (1986) showed that NDVI maintains strong correlations with soil moisture across Ethiopia, enabling use of RS composites to monitor green-up and senescence of crops, and noted differences in lag

times of NDVI signals between green-up and senescence. Fourier analysis of NDVI time-series has refined analyses further, permitting discrimination of vegetation types (Olsson and Eklundh 1994) because annual phenological cycles generally correlate to unimodal or bimodal distributions. Azzali and Menenti (2000) refined vegetation classification further by clustering amplitudes (maximum variation around mean NDVI) and phases (timing of maximum NDVI) at each location, across several time steps from Fourier analyses.

1.3 Remote sensing and disease

Relatively little use has been made of RS data for refining ecological knowledge of temporal dynamics of enviro-climatic processes affecting human disease occurrence. Work by Anyamba *et al.* (2002) on Rift Valley fever (RVF) outbreaks is an exception, analysing time series of monthly NDVI composites for anomalous rain events, since RVF outbreaks are associated with increases in areas suitable for mosquito breeding. Anomalies were identified pixel by pixel for periods in which a pixel's average monthly value exceeded the 19-year mean over three consecutive months. Although these anomalies occurred more frequently than major RVF outbreaks, major outbreaks were strongly associated with anomalies over the period analysed.

Generally, the temporal component of RS information has been used to refine estimates of areas of occurrence or potential occurrence (Rogers *et al.* 1996, Hay *et al.* 1998). Within this literature, one focus has been on using RS data in models for predicting disease occurrences, such as in outbreaks of hantavirus pulmonary syndrome linking with El Niño events the previous year (Engelthaler *et al.* 1999, Boone *et al.* 2000, Glass *et al.* 2000). RS data analyses have also been important inputs to models for understanding environmental preconditions for malaria transmission (Rogers *et al.* 2002). In all of these cases, however, hosts and transmission modes are well documented.

When hosts and transmission modes are not known, however, RS data have been little explored, perhaps because such information is considered to be 'prerequisite for all epidemiological applications of remote sensing' (Hay *et al.* 1997). In the case of filoviruses, about 18 human or primate disease outbreaks are known to have been caused by Ebola or Marburg viruses since 1967. Their occurrences have been without obvious pattern, suggesting that filovirus transmission to humans is rare, and that significant random elements may be involved (Leroy *et al.* 2004, Walsh *et al.* 2005). This lack of predictability, particularly in temporal dimensions, as well as nearly complete lack of information regarding their ecology and natural history, has hindered research on these viruses. Monath (1999) first considered the ecology of filoviruses, plotting locations of Ebola outbreaks against annual precipitation patterns. Tucker *et al.* (2002) and Pinzon *et al.* (2004) explored further links between filovirus-caused disease outbreaks and precipitation by analysing AVHRR NDVI time-series associated in time and space with Ebola outbreaks. Their research concluded that Ebola outbreaks were correlated with 'sudden climate changes from drier to wetter conditions' four months prior to outbreaks (Tucker *et al.* 2002, Pinzon *et al.* 2004). Our research differs from the work of Tucker *et al.* (2002) and Pinzon *et al.* (2004) in both data and methodology. With 10-day composite images, this article investigates the utility of wavelet analysis to detect environmental change across varying time scales not examined in their studies. We explore the hypothesis that links between climate and filovirus disease outbreaks exist, and that these links can be observed by relating time-specific RS data to disease outbreaks. We focus not only on the identification of associations but also on testing the generality of patterns by means of replicate analyses. We consider this contribution to be a first exploration of a more

quantitative approach to understanding temporal correlates of disease transmission, even in poorly known systems.

2. Methods

To examine linkages between RS data and a common climate signal preceding an outbreak, we analysed a time series of 10-day composite NDVI values from the NOAA/NASA Pathfinder AVHRR dataset (Agbu and James 1994). We assembled a 20-year series (1981–2001) of this data set for all of Africa, which was complete, save for a three-month period in 1994. This broad data resource was then probed to extract time series for pixels corresponding to known outbreak sites.

We analysed all filovirus disease outbreaks (Figure 1) that met a series of criteria: (1) outbreaks occurred within the temporal range of the Pathfinder dataset (July 1981–September 2001); (2) outbreaks fell outside of the three-month period for which data were unavailable; finally, (3) date of transmission from reservoir to humans or other primates was sufficiently known (Georges, 1999). In the end, five outbreaks remained for analysis (Table 1): two of Marburg virus, and three of Ebola virus (Figure 1). As these two virus genera form a monophyletic clade, and likely share a common host clade (Peterson *et al.* 2004a,b), we treated sites for the two genera similarly.

Spatial and temporal uncertainties within the outbreak data are inherent, and accounting for them is necessary for accurately interpreting the results of our analysis. The uncertainty stems from precisely identifying times and locations where human index cases contacted the virus' host. We outlined a maximum possible spatial extent for each

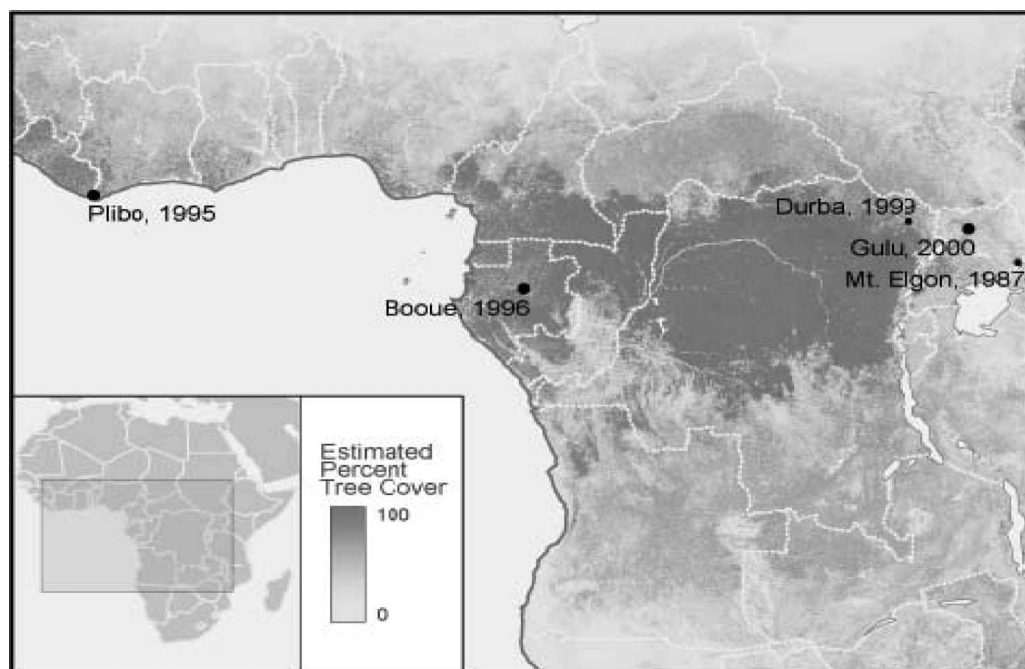


Figure 1. Spatial distribution of the five African filovirus outbreaks analysed herein, shown atop a satellite-derived estimate of tree cover (Defries *et al.* 2000) to provide a sense of the vegetation patterns in the region.

Table 1. Locations, dates and literature sources for filovirus-caused hemorrhagic fever occurrences.

Site	Country	Dates	Criteria number			Reference
			1	2	3	
1. Sinoia Caves	Zimbabwe	February 1976				Peterson <i>et al.</i> 2006
2. Nzara	Sudan	June–November 1976				World Health Organisation 1978a
3. Yambuku	DRC	September–October 1976				World Health Organisation 1978b
4. Bonduni	DRC	June 1977				Heymann <i>et al.</i> 1980
5. Nzara	Sudan	July–October 1979				Baron <i>et al.</i> 1983
6. Nzoia or Mt. Elgon	Kenya	January 1980				Smith <i>et al.</i> 1982
7. Mt. Elgon	Kenya	August 1987	X	X	X	Peters <i>et al.</i> 1997, World Health Organisation, 2005
8. Tai National Park	Côte d'Ivoire	November 1994	X			Le Guenno <i>et al.</i> 1995, Peters <i>et al.</i> 1997, Formenty <i>et al.</i> 1999
9. Minkebe, Mekouka, and/or Andock	Gabon	December 1994–February 1995	X			Georges <i>et al.</i> 1999
10. Kikwit	DRC	January–July 1995	X			Khan <i>et al.</i> 1999
11. Plibo	Côte d'Ivoire or Liberia	December 1995	X	X	X	World Health Organisation, 1995
12. Mayibout	Gabon	February 1996	X	X		Georges <i>et al.</i> 1999
13. Booue	Gabon	July 1996–March 1997	X	X	X	Georges <i>et al.</i> 1999
14. Durba	DRC	April 1999–September 2000	X	X	X	Bertherat <i>et al.</i> 1999, Zeller, 2000
15. Gulu	Uganda	October 2000–February 2001	X	X	X	Centers for Disease Control and Prevention, 2001
16. Ekata	Gabon and DRC	December 2001–2002				Leroy <i>et al.</i> 2002
17. Yambio	Sudan	May 2004				World Health Organisation 2004
18. Uige Province	Angola	October 2004				Centers for Disease Control and Prevention, 2005

Note: Criteria are as follows: (1) outbreaks occurred between July 1981 and 3 September 2001, (2) outbreaks that not have occurred in the three-month gap in the Pathfinder 4 data and (3) outbreak timing and location known with sufficient accuracy.

outbreak, either based on the literature or delineated via consultation with epidemiologists who studied the outbreaks, based on movements of the index case in the 5–20 days preceding onset of symptoms (Peterson *et al.* 2006). These polygons provide a standardized unit of analysis for examining climatic variation across the common locations where host-to-human transmission is most likely to have occurred for each outbreak using the RS data.

The spatial resolution of the Pathfinder dataset is 8 km. Temporal uncertainty springs from the process used to create the 10-day maximum NDVI composite images used as input to the wavelet analyses. The maximum NDVI value for a pixel can come from any day in the 10-day period, so the lag of the values for the same pixel in two adjacent time periods may have occurred anywhere from one day apart to 19 days apart, although the average is ~ 10 days, and we will speak in these terms throughout this article. The spatial averaging across pixels within outbreak polygons (see below) should help to reduce this uncertainty and keep temporal steps closer to 10 days.

The final datasets analysed consisted of NDVI time-series of spatial mean values across all pixels in outbreak polygons for all 10-day periods in the data set. Here, we present the results for the 2 years preceding each outbreak, under the assumption that any relevant environmental signals occur within that time frame. Based on the size of outbreak polygons, 14–44 pixels (896–2 816 km²) were averaged into spatial mean NDVI values. Spatial means and variances in each time period were compared to ensure that the mean adequately represented the variation within the extent of outbreak polygons.

Wavelet analysis is a means of examining variation across different scales although focusing on how different scales influence observed signals at particular points in the signal. This approach offers benefits over more traditional methods of signal processing (e.g. Fourier transform) by determining not only which scales are observed within the signal but also where in the signal the different scales are active. For example, suppose a time series consists of two modes (a diurnal and an annual cycle), wavelets allow us to determine when in the signal each of the different cycles is dominant. During certain times, the diurnal cycle might be more important, whereas at others the annual cycle might be more important. Although the signal can consist of any type of data (spatial or temporal), we focus here on temporal phenomena. More extensive explanations of wavelet analysis are available elsewhere (Lau and Weng 1995, Torrence and Compo 1998, Percival *et al.* 2004); however, for the sake of completeness, we offer a brief review.

A wavelet transform works by examining the variation of a ‘mother’ wavelet as it is dilated and translated through the original time series. The dilation determines the scale (resolution), and the translation allows the determination of where in the time series is influenced by that scale. The mother wavelet used here is the Morlet wavelet. The wavelet coefficients are obtained by convolving the mother wavelet through different levels of dilation (scales), and progressing that scale through each point in the time series:

$$W(a, b) = \frac{1}{\sqrt{1}} \int_{-\infty}^{\infty} f(x) \overline{\psi\left(\frac{x-b}{a}\right)} dx$$

where $W(a, b)$ are the wavelet coefficients at scale a and location b within the time-series $f(x)$, and the overbar indicates the complex conjugate. These coefficients represent the relative importance of that scale to that particular point in time. We attempted to determine the extent to which disease outbreaks are associated with climatic anomalies in the RS data. Therefore, we defined a scale-wise anomaly in the NDVI signal as any time that the absolute value of the wavelet coefficient departs by > 2 standard deviations from the mean of the coefficients for that particular scale. To examine temporal dynamics

surrounding anomalies associated with various scales, we took the inverse transform of the coefficients after setting the coefficients from all other scales to zero. This is a band-pass filter of the wavelet coefficients, and is achieved using the discrete wavelet transform. This inverse-transformed, filtered signal represents the NDVI signal as observed at a particular scale (e.g. monthly), so we can examine variability associated with anomalies without looking at the high-frequency noise in the signal or the variability induced by longer time scales, such as annual cycles in vegetation.

3. Results

Seasonal fluctuations were evident in the NDVI time-series. Although the suggestion has been made (Tucker *et al.* 2002, Pinzon *et al.* 2004, 2005) that filovirus disease outbreaks occur principally four months following dry-to-wet transitions, this pattern is not universal (see, e.g. the outbreak at Gulu). As such, we believe that more complex explanations will be necessary before climate-outbreak connections are clearly identified.

Figure 2 presents a step-by-step illustration of the results for the Gulu, Uganda, outbreak. The wavelet analysis was performed over the entire 20 years of NDVI data, but for clarity in the illustrations, we show only the 2 years preceding the start of the outbreak. The top panel shows the spatially averaged NDVI time series, with the standard deviations illustrating how representative the spatial mean is at each time. It is clear that examination of the NDVI time series *per se* is not illustrative, i.e. no clear change is apparent in the NDVI signal preceding the outbreak.

The second panel shows the wavelet modulus of the NDVI time series. The vertical axis represents the temporal scale of the wavelet decomposition, with larger scales at the top. As scale increases, the ability to locate that scale accurately at a particular time decreases, so the blocks in the figure increase in width horizontally. Lighter colours indicate greater importance of that scale at that particular time. Immediately prior to the outbreak, significant activity is noticeable at smaller time scales.

To examine the importance and temporal distribution of this scale-dependent energy, the third panel plots the wavelet coefficients at the third level of decomposition (equivalent to a 20-day scale of temporal phenomena). On this plot, brighter colours at the third level of decomposition are associated with significant variability at this scale. Although little variation in the wavelet coefficients is evident more generally at this scale over this time period, near the time of the outbreak, large amounts of oscillation are visible around the mean. Particularly, extreme behaviours ($2 +$ standard deviations from the mean) are associated with large changes in the NDVI time series at that scale and are henceforth referred to as scale-wise anomalies.

To examine the relationships between anomalous NDVI values at certain time scales and observed variability in the NDVI time series, we used the inverse wavelet transform to calculate the variation in NDVI at this time scale (fourth panel). The two periods identified as containing scale-wise anomalies preceding the outbreak correspond to very minor changes in the NDVI signal, details easily lost in examination of the full NDVI time series. This analysis suggests that no clear and simple association with some environmental signal (such as the 'dry-to-wet' transition) exists, but rather that the association is with *extreme* conditions manifested at specific time scales. Hence, although the ecological interpretation of this result is not completely clear and interpretable, the anomalies are easily identifiable.

In this study, we analysed a broad range of time scales. Figure 3 illustrates this diversity, showing wavelet coefficients and scale-wise anomalies for the Uganda outbreak.

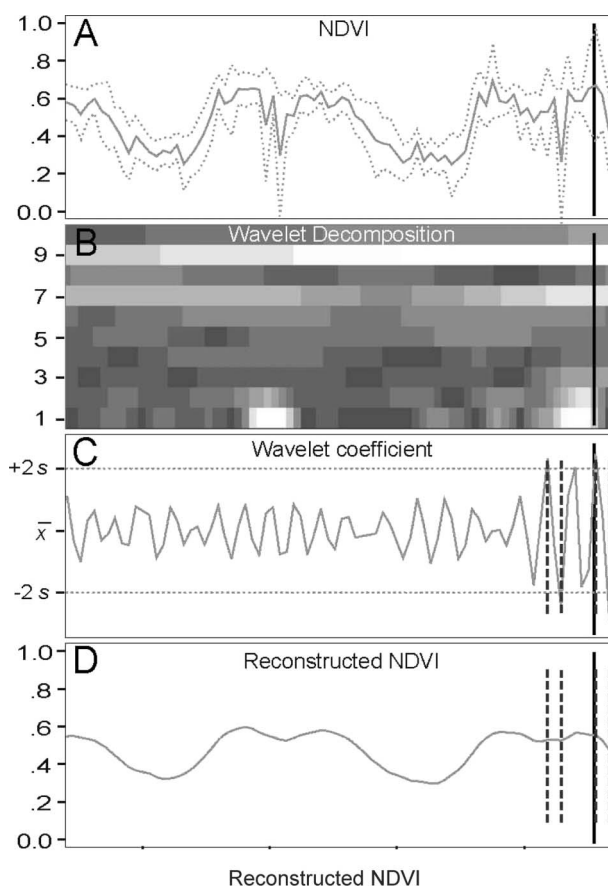


Figure 2. Exemplar wavelet analysis for the 2000 Gulu, Uganda, outbreak (the outbreak date is shown as a solid vertical black line in each panel). (A) Time series of the spatial mean (solid line) is shown with variance of NDVI across pixels within outbreak polygons (broken lines). (B) The wavelet modulus shows variations across time-scales (vertical axis, with the finest temporal scale at the bottom, and the broadest scales at the top), decomposed from the spatial mean NDVI values through time (horizontal axis). Brighter colours indicate times of increased weighting at that time scale. (C) The coefficient for the third level of decomposition shows anomalies (dashed-vertical lines) defined as when the coefficient exceeds a threshold of ± 2 standard deviations. (D) A reconstructed (band-passed filtered) NDVI signal from the inverse wavelet transform of the third level.

The only time scale at which a consistent association existed between scale-wise anomalies in the NDVI signal and the occurrence of an outbreak was the third, which relates to phenomena occurring at a 20-day scale. Indeed, scale-wise anomalies at the third level occurred 1 to 3 weeks preceding 4 of the 5 outbreaks analysed (Figure 4). In one case (Plibo, Panel B in Figure 4), although a scale-wise anomaly was not observed preceding the outbreak, such an anomaly is indicated following the surmised outbreak date closely, by 1–10 days.

It is important to note that not all scale-wise anomalies in the RS time series are accompanied by known outbreaks. This result is expected for several reasons, most revolving around the rare, chance nature of filovirus transmission. That is, although anomalies may represent times of special opportunity for transmission, given the rare nature of filovirus-caused disease, not every opportunity results in transmission to

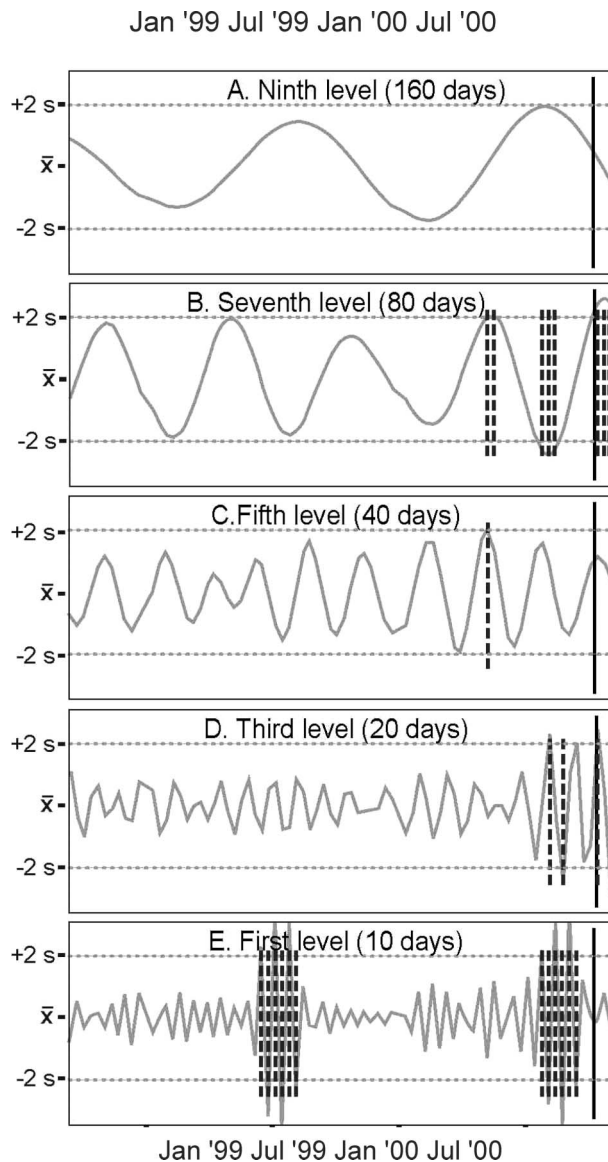


Figure 3. Example of wavelet analysis results (for Gulu, Uganda, 2000 outbreak), showing anomalies identified at each time scale. The horizontal axis represents time preceding outbreaks (solid vertical line). The vertical axis shows time series of wavelet coefficient values (solid lines), in relation to ± 2 standard deviations (dotted-horizontal line). (A) ninth level of decomposition (160 days), (B) seventh (80 days), (C) fifth (40 days), (D) third (20 days) and (E) first (10 days).

humans. The possibility also exists of human cases that are not documented or reported to the wider community.

4. Discussion and conclusions

A thorough understanding of spatial and temporal correlations of disease transmission events can be critical in understanding how the disease is transmitted. For example, in

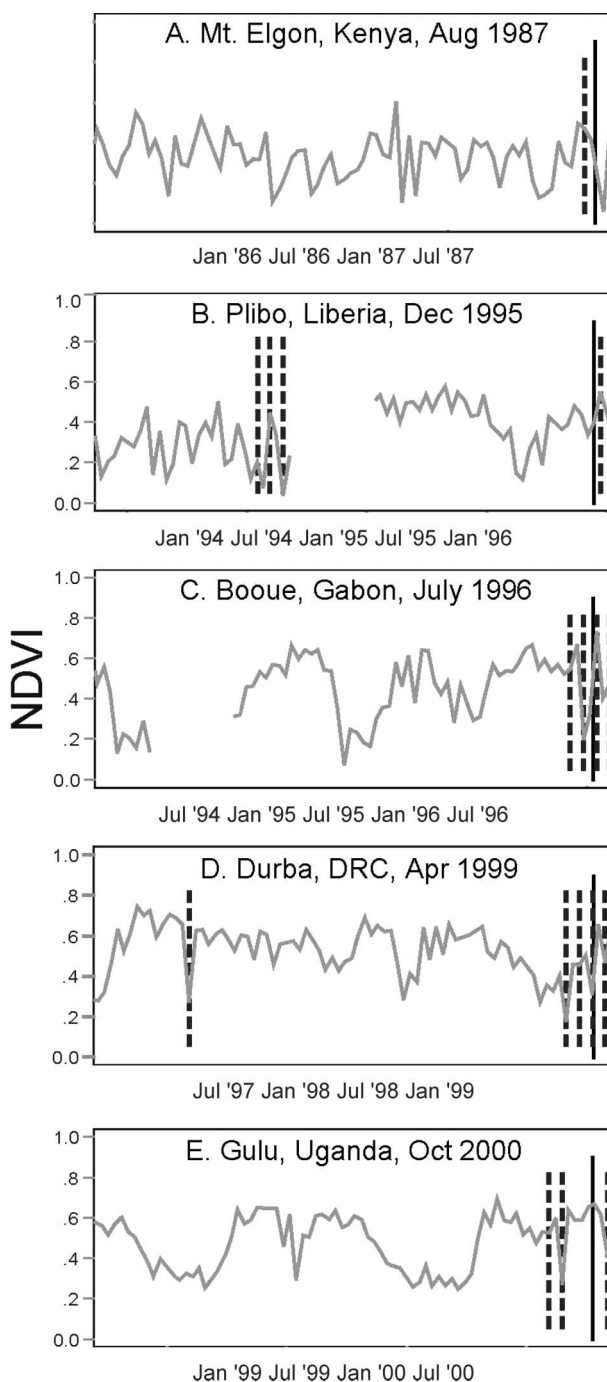


Figure 4. Time series of mean NDVI for each of the five filovirus outbreaks analysed. Anomalies at the third level of decomposition are dashed vertical lines at the median date of a 20-day period, shown relative to outbreaks (solid vertical lines).

research into the dynamics of hantavirus transmission in North America, a critical observation was the one-year lag between elevated rainfall in the southwestern USA and abundant hantavirus transmission a year later (Hjelle and Glass 2000, Yates *et al.* 2002). This association led eventually to identification of host rodent population dynamics being elevated by abundant food, and altered behaviour (increased commensalism with humans) in the following year of lower resource availability, as key factors in hantavirus transmission (Yates *et al.* 2002). This article on filoviruses follows our previous efforts to identify factors important over space (Peterson *et al.* 2004a), in an effort to identify key temporal scales at which trigger events – if any exist – act in filovirus transmission. In the case of the filoviruses, we found a close association between extreme events on a temporally averaged scale of 20 days, one to three weeks prior to known filovirus transmission events. All five filovirus outbreaks were associated with such extreme events, although the time lag in one case was different. This association is suggestive of some sort of trigger event at relatively short time scales at least increasing the probability of filovirus transmission to humans. Monath (1999) wrote that ‘there are no data to suggest that Ebola outbreaks have been associated with an unusual “bloom”, or with a periodicity linked to weather phenomena’, and then that disease vectors or hosts may have altered behaviour ‘linked to high rainfall and associated environmental changes’. The fact that scale-wise anomalies occur at a consistent time interval demonstrates a link between outbreaks and climatic processes. That anomalies do not fit a consistent trend in the NDVI signal (i.e. dry to wet, wet to dry, peak dryness, or peak wetness) suggests that the climatic processes driving the anomalies may not be fully understood through NDVI data alone. Although anomalies appear more frequently than have known filovirus outbreaks, previous studies of climate anomalies and RVF had similar results (Anyamba *et al.* 2002). This result is acceptable given that a broader suite of preconditions must be met for disease outbreaks to occur: presence of humans, sufficient interaction between humans and the reservoir host, etc., in addition to climatic dynamics.

The question then becomes, what does this variability in wavelet coefficients ‘look like’ with respect to the original NDVI time series? Previous studies identified the ‘dry-to-wet’ transition as a key focus for filovirus transmission to humans (Tucker *et al.* 2002, Pinzon *et al.* 2004), and others have noted that outbreaks tend to initiate late in the calendar year (Monath 1999). Our examination, however, indicates that the situation is more complex than these simple summaries. Conceptualizing a climatic process at a 20-day time-scale can be difficult for those familiar with climate patterns in temperate latitudes: diurnal climatic processes are strongly correlated to direct solar radiation; weekly climate patterns are often correlated to synoptic scale weather systems; and seasonal climate patterns are easily explained by the Earth’s axial tilt and the resulting influence on global circulation patterns via alterations to the jet stream and the Inter Tropical Convergence Zone. One of the primary difficulties associated with meteorological and climatic analysis is to determine to what extent these processes (and others operating at different time-scales) manifest themselves locally. All processes are present at all times in all locations, and at any given time, a process operating at a particular time-scale may have more importance on the local environment (i.e. by inducing a dramatic positive or negative deviation from the mean).

Characterizing the mechanics of climatic processes at a 20-day time-scale is not easily achieved with only one data input (NDVI in this case). To understand the processes determining local climatic behaviour, it would be best to incorporate more climatic variables, such as soil moisture and evapotranspiration, which would help explain how the vegetation response detected with the NDVI data is occurring. However, the primary purpose of this article is to identify relevant time-scales of the process, so that more research focus can be placed on processes that actually manifest themselves at that scale.

How might a lag time of a few weeks manifest itself in increased probability of filovirus transmission? Of course, the easy interpretation would be a population response in an arthropod vector, as has been suggested for malaria transmission, but strong arguments have been made against a role for arthropod vectors in filovirus transmission (Peterson *et al.* 2004b). Given that the time frame involved is too short for vertebrate host population responses, other possible explanations would include either increased viral populations circulating in hosts, or changes in host behaviour that might increase probability of contact with humans.

As a hypothetical example, consider the 'dry-to-wet' transition identified by previous researchers (Tucker *et al.* 2002, Pinzon *et al.* 2004). Perhaps it is not a matter of total precipitation and a regional/seasonal transition, but rather some scenario like the following: during a time when root-zone soil moisture may be limited, a specific amount of precipitation occurs that increases surface water, which might in turn, increase the number of individuals within the reservoir host population. Then, an extended dry-down period follows, in which the vegetation must begin to access water deeper in the soil column, which is already depleted; as such, the vegetation may begin to exhibit water stress, causing a response in the NDVI signal (at ~ 20 days prior to outbreaks). Because the numbers of host individuals are elevated, they begin to disperse away from the original location, increasing the likelihood of contact with humans. The purpose of this example is not to suggest that this is the actual mechanism responsible, but rather that because the relevant time scale has been determined, we can now attempt to identify biophysical mechanisms more directly responsible for increases in disease transmission associated with anomalies at that time scale.

The previous time-series analyses of filovirus transmission events (Tucker *et al.* 2002, Pinzon *et al.* 2004, 2005) were based on data from the same AVHRR NDVI 8 km data resource as we have used, although the details of their preparation and processing of these data resources are unspecified and may differ from those followed here. These previous studies produced results that contrast in important ways with our own: through scale-wise analysis, we were able to isolate consistent variability at the 20-day scale preceding outbreaks, whereas previous results relied heavily on absolute differences in the four-month periods preceding outbreaks (Tucker *et al.* 2002), or in deviations from the seasonal means (Pinzon *et al.* 2004). Several reasons exist for these differences: (1) unspecified data manipulations in preparation of their version of the AVHRR NDVI data set may be responsible for some variations in patterns; (2) their version of the AVHRR NDVI data set was resolved temporally only to monthly periods, which prevents detection of events at the shorter time scales that were our result; (3) their patterns were 'detected' (Tucker *et al.* 2002) without a quantitative methodology, rather being inferred *a posteriori* based on visual inspection (to the best of our knowledge) of time series, whereas our anomalies were detected independent of knowledge of the timing of outbreaks.

Given the limited number of known filovirus outbreaks to date it is not possible to validate our results statistically, but their generality could be tested in a number of ways. Testing additional filovirus outbreaks could be accomplished using the NASA Global Inventory Monitoring and Modeling Systems (GIMMS) dataset, a revised AVHRR 8 km 10-day composite NDVI dataset, which would enable the inclusion of the three additional outbreaks that coincide with the 3-month gap in the Pathfinder data, as well as other outbreaks that have occurred since 2001. However, it should be noted that addition of these other outbreaks would not increase the statistical significance of the methodology, as the number of outbreaks are still too few for standard tests of significance. Again, the

primary purpose of this article is to suggest a methodology for determining whether a climatic signal can be observed prior to the outbreaks so that future work can focus on the actual biophysical processes associated with the outbreaks.

More to the point of understanding filovirus transmission dynamics, integration of results from spatial studies (Peterson *et al.* 2004a) with the temporal results developed herein would go a long way towards understanding the degree to which signals can be distinguished among the 'noise' of the random and rare factors governing filovirus transmission. More generally still, wavelet analysis offers a fascinating new approach to illuminating temporal – and potentially spatial as well – aspects of disease transmission, and as such merits further exploration beyond this first effort.

Acknowledgements

The authors thank David Vieglais, Kevin Ruland and Rob Gales, for their help with manipulating the RS data. Additional thanks to Karl Johnson, Jim Mills and Darin Carroll for their sage advice and input. Data used were generously provided by the Earth Observing System Pathfinder Program of NASA's Mission to Planet Earth, in cooperation with the National Oceanic and Atmospheric Administration. Work was done under a contract from the US Department of Defense.

References

- Agbu, P.A. and James, M.E., 1994. *The NOAA/NASA Pathfinder AVHRR Land Data Set User's Manual*, Goddard Distributed Active Archive Center, NASA, Goddard Space Flight Center, Greenbelt.
- Anyamba, A., Linthicum, K.J., Mahoney, R., Tucker, C.J., and Kelley, P.W., 2002. Mapping potential risk of Rift Valley Fever outbreaks in African savannas using vegetation index time series data. *Photogrammetric Engineering and Remote Sensing*, 68, 137–145.
- Azzali, S. and Menenti, M., 2000. Mapping vegetation-soil-climate complexes in southern Africa using temporal Fourier analysis of NOAA-AVHRR NDVI data. *International Journal of Remote Sensing*, 21, 973–996.
- Baron, R.C., McCormick, J.B., and Zubeir, O.A., 1983. Ebola virus disease in southern Sudan: hospital dissemination and intrafamilial spread. *Bulletin of the World Health Organization*, 61, 997–1003.
- Bausch, D.G., Borchert, M., Grein, T., Roth, C., Swanepoel, R., Libande, M.L., Talarmin, A., Bertherat, E., Muyembe-Tamfum, J.-J., Tugume, B., Colebunders, R., Kondé, R.M., Pirard, P., Olinda, L.L., Rodier, G.R., Campbell, P., Tomori, O., Ksiazek, T.G. and Rollin, P.E., 2003. Risk factors for Marburg hemorrhagic fever, democratic republic of the Congo. *Emerging Infectious Diseases*, 9, 1531–1537.
- Beck, L.R., Lobitz, B.M., and Wood, B.L., 2000. Remote sensing and human health: new sensors and new opportunities. *Emerging Infectious Diseases*, 6, 217–226.
- Bertherat, E., Talarmin, A., and Zeller, H., 1999. Democratic republic of the Congo: between civil war and the Marburg virus. International Committee of Technical and Scientific Coordination of the Durba Epidemic. *Médecine Tropicale*, 59, 201–204.
- Boone, J.D., McGwire, K.C., Otteson, E.W., Debaca, R.S., Kuhn, E.A., Villard, P., Brussard, P.F., and St Jeor, S.C., 2000. Remote sensing and geographic information systems: charting Sin Nombre Virus infections in deer mice. *Emerging Infectious Diseases*, 6, 248–258.
- Breman, J.G., Johnson, K.M., Van der Groen, G., Robbins, C.B., Szczeniowski, M.V., Ruti, K., Webb, P.A., Meier, F., Heymann, D.L. and Teams, E.V.S., 1999. A search for Ebola Virus in animals in the Democratic Republic of the Congo and Cameroon: ecologic, virologic, and serologic surveys, 1979–1980. *Journal of Infectious Disease*, 179, S139–S147.
- Centers for Disease Control and Prevention, 2001. Outbreak of Ebola hemorrhagic fever Uganda, August 2000–January 2001. *Morbidity and Mortality Weekly Report*, 50, 73–77.
- Centers for Disease Control and Prevention, 2005. Outbreak of Marburg virus hemorrhagic fever, Angola, October 1, 2004–March 29, 2005. *Morbidity and Mortality Weekly Report*, 54, 308–309.
- Conrad, J.L., Isaacson, M., Smith, E.B., Wulff, H., Crees, M., Geldenhuys, P., and Johnston, J., 1978. Epidemiologic investigation of Marburg virus disease, Southern Africa, 1975. *American Journal of Tropical Medicine and Hygiene*, 27, 1210–1215.

- Cracknell, A.P., 1997. *Advanced very high resolution radiometer: AVHRR*. London: Taylor and Francis.
- Curran, P.J., Atkinson, P.M., Foody, G.M., and Milton, E.J., 2000. Linking remote sensing, land cover and disease. *Advances in Parasitology*, 47, 37–80.
- Defries, R.H.M., Townshend, J.R.G., Janetos, A.C., and Loveland, T.R., 2000. Africa. *AVHRR continuous fields tree cover project*. College Park, University of Maryland, Department of Geography.
- Engelthaler, D.M., Mosley, D.G., Cheek, J.E., Levy, C.E., Komatsu, K.K., Ettestad, P., Davis, T., Tanda, D.T., Miller, L., Frampton, J.W., Porter, R. and Bryan, R.T., 1999. Climatic and environmental patterns associated with Hantavirus Pulmonary Syndrome, Four Corners Region, United States. *Emerging Infectious Diseases*, 5, 87–94.
- Formenty, P., Boesch, C., Wyers, M., Steiner, C., Donati, F., Dind, F., Walker, F., and Le Guenn, B., 1999. Ebola virus outbreak among wild chimpanzees living in a rain forest of Cote d'Ivoire. *Journal of Infectious Diseases*, 179, S120–S126.
- Georges, A.-J., Leroy, E.M., Renaut, A.A., Benissan, C.T., Nabias, R.J., Ngoc, M.T., Obiang, P.I., Lepage, J.P.M., Bertherat, E.J., Bénoni, D.D., Wickings, E.J., Amblard, J.P., Lansoud-Soukate, J.M., Milleliri, J.M., Baize, S. and Georges-Courbot, M.-C., 1999. Ebola hemorrhagic fever outbreaks in Gabon, 1994–1997: epidemiologic and health control issues. *Journal of Infectious Diseases*, 179, S65.
- Glass, G.E., Cheek, J.E., Patz, J.A., Shields, T.M., Doyle, T.J., Thoroughman, D.A., Hunt, D.K., Ensore, R.E., Gage, K.L., Irland, C., Peters, C.J. and Bryans, R., 2000. Using remotely sensed data to identify areas at risk for Hantavirus Pulmonary Syndrome. *Emerging Infectious Diseases*, 6, 238–247.
- Hay, S.I., Packer, M.J., and Rogers, D.J., 1997. The impact of remote sensing on the study and control of invertebrate intermediate hosts and vectors for disease. *International Journal of Remote Sensing*, 18, 2899–2930.
- Hay, S.I., Snow, R.W., and Rogers, D.J., 1998. Predicting malaria seasons in Kenya using multitemporal meteorological satellite sensor data. *Transactions of the Royal Society of Tropical Medicine and Hygiene*, 92, 12–20.
- Henricksen, B.L. and Durkin, J.W., 1986. Growing period and drought early warning in Africa using satellite data. *International Journal of Remote Sensing*, 7, 1583–1608.
- Heymann, D.L., Weisfeld, J.S., Webb, P.A., Johnson, K.M., Cairns, T., and Berquist, H., 1980. Ebola hemorrhagic fever: Tandala, Zaire, 1977–1978. *Journal of Infectious Diseases*, 142, 372–376.
- Hjelle, B. and Glass, G.E., 2000. Outbreak of hantavirus infection in the Four Corners region of the United States in the wake of the 1997–1998 El Niño-Southern Oscillation. *Journal of Infectious Diseases*, 181, 1569–1573.
- Holben, B.N., 1986. Characteristics of maximum-value composite images from temporal AVHRR data. *International Journal of Remote Sensing*, 7, 1417–1434.
- Holben, B.N. and Justice, C., 1981. An examination of spectral band ratioing to reduce the topographic effect on remotely sense data. *International Journal of Remote Sensing*, 2, 115–133.
- James, M.E. and Kalluri, S.N.V., 1994. The Pathfinder AVHRR land data set: an improved coarse resolution data set for terrestrial monitoring. *International Journal of Remote Sensing*, 15, 3347–3363.
- Justice, C.O., Holben, B.N., and Gwynne, M.D., 1986. Monitoring East African vegetation using AVHRR data. *International Journal of Remote Sensing*, 7, 1453–1474.
- Khan, A.S., Tshioko, F.K., Heymann, D.L., Le Guenno, B., Nabeth, P., Kerstiens, B., Fleerackers, Y., Kilmarx, P.H., Rodier, G.R., Nkuku, O., Rollin, P.E., Sanchez, A., Zaki, S.R., Swanepoel, R., Tomori, O., Nichol, S.T., Peters, C.J., Muyembe-Tamfum, J.J. and Ksiazek, T.G., 1999. The reemergence of Ebola hemorrhagic fever, Democratic Republic of the Congo, 1995. *Journal of Infectious Diseases*, 179 (Suppl 1), S76–S86.
- Lau, K.-M. and Weng, H., 1995. Climate signal detection using wavelet transform: how to make a time series sing. *Bulletin of the American Meteorological Society*, 76, 2391–2402.
- Le Guenno, B., Formenty, P., Wyers, M., Gounon, P., Walker, F., and Boesch, C., 1995. Isolation and partial characterization of a new strain of Ebola virus. *The Lancet*, 345, 1271–1274.
- Leirs, H., Mills, J.N., Krebs, J.W., Childs, J.E., Akaibe, D., Woollen, N., Ludwig, G., Peters, C.J., and Ksiazek, T.G., 1999. Search for the Ebola virus reservoir in Kikwit, Democratic Republic of the Congo: reflections on a vertebrate collection. *Journal of Infectious Disease*, 179, S155–S163.

- Leroy, E.M., Kumulungui, B., Pourrut, X., Rouquet, P., Hassanin, A., Yaba, P., Dèlicat, A., Paweska, J.T., Gonzalez, J.-P. and Swanepoel, R., 2005. Fruit bats as reservoirs of Ebola virus. *Nature*, 438, 575–576.
- Leroy, E.M., Rouquet, P., Formenty, P., Souquière, S., Kilbourne, A., Froment, J.-M., Bermejo, M., Smit, S., Karesh, W., Swanepoel, R., Zaki, S.R. and Rollin, P.E., 2004. Multiple Ebola Virus transmission events and rapid decline of Central African wildlife. *Science*, 303, 387–390.
- Leroy, E.M., Souquiere, S., Rouquet, P., and Drevet, D., 2002. Re-emergence of ebola haemorrhagic fever in Gabon. *The Lancet*, 359, 712.
- Maiden, M.E. and Greco, S., 1994. NASA's Pathfinder data set programme: land surface parameters. *International Journal of Remote Sensing*, 15, 3333–3345.
- Mills, J.N. and Childs, J.E., 1998. Ecologic studies of rodent reservoirs: their relevance for human health. *Emerging Infectious Diseases*, 4, 529–537.
- Monath, T.P., 1999. Ecology of Marburg and Ebola viruses: speculations and directions for future research. *Journal of Infectious Disease*, 179, S127–S138.
- Murphy, F.A., Van der Groen, G., Whitfield, S.G., and Lange, J.V., 1978. Ebola and Marburg virus morphology and taxonomy. In: S.R. Pattyn, ed. *International colloquium on Ebola virus infection and other haemorrhagic fevers*, Antwerp, 1977. *Ebola virus haemorrhagic fever*. Amsterdam: Elsevier/North-Holland Biomedical Press.
- Olsson, L. and Eklundh, L., 1994. Fourier Series for analysis of temporal sequences of satellite sensor imagery. *International Journal of Remote Sensing*, 15, 3735–3741.
- Percival, D.B., Wang, M., and Overland, J.E., 2004. An introduction to wavelet analysis with applications to vegetation time series. *Community Ecology*, 5, 19–30.
- Peters, C.J. and Olshaker, M., 1997. *Virus hunter: thirty years of battling hot viruses around the World*. New York: Anchor Books Doubleday.
- Peterson, A.T., Bauer, J.T., and Mills, J.N., 2004a. Ecologic and geographic distribution of filovirus disease. *Emerging Infectious Diseases*, 10, 40–47.
- Peterson, A.T., Carroll, D.S., Mills, J.N., and Johnson, K.M., 2004b. Potential mammalian filovirus reservoirs. *Emerging Infectious Diseases*, 10, 2073–2081.
- Peterson, A.T., Lash, R.R., Carroll, D., and Johnson, K.M., 2006. Geographic potential for outbreaks of Marburg hemorrhagic fever. *American Journal of Tropical Medicine and Hygiene*, 75, 9–15.
- Pinzon, J.E., Wilson, J.M., and Tucker, C.J., 2005. Climate-based health monitoring systems for eco-climatic conditions associated with infectious diseases. *Bulletin de la Société de Pathologie Exotique*, 98, 239–243.
- Pinzon, J.E., Wilson, J.M., Tucker, C.J., Arthur, R., Jahrling, P.B., and Formenty, P., 2004. Trigger events: enviroclimatic coupling of Ebola haemorrhagic fever outbreaks. *American Journal of Tropical Medicine and Hygiene*, 71, 664–674.
- Rogers, D.J., Hay, S.I., and Packer, M.J., 1996. Predicting the distribution of tsetse flies in West Africa using temporal Fourier processed meteorological satellite data. *Annals of Tropical Medicine and Parasitology*, 90, 225–241.
- Rogers, D.J., Randolph, S.E., Snow, R.W., and Hay, S.I., 2002. Satellite imagery in the study and forecast of malaria. *Nature*, 415, 710–715.
- Smith, D.H., Johnson, B.K., Isaacson, M., Swanepoel, R., Johnson, K.M., Killey, M., Bagshawe, A., Siongok, T., and Keruga, W.K., 1982. Marburg-virus disease in Kenya. *The Lancet*, 319, 816–820.
- Torrence, C. and Compo, G.P., 1998. A practical guide to wavelet analysis. *Bulletin of the American Meteorological Society*, 79, 61–78.
- Townshend, J.R.G. and Justice, C.O., 1986. Analysis of the dynamics of African vegetation using the normalized difference vegetation index. *International Journal of Remote Sensing*, 7, 1435–1474.
- Townshend, J.R.G. and Tucker, C.J., 1984. Objective assessment of advanced very high resolution radiometer data for land cover mapping. *International Journal of Remote Sensing*, 5, 497–504.
- Tucker, C.J., 1979. Red and photographic infrared linear combinations for monitoring vegetation. *Remote Sensing of Environment*, 8, 127–150.
- Tucker, C.J., Wilson, J.M., Mahoney, R., Anyamba, A., Linthicum, K., and Myers, M.F., 2002. Climatic and ecological context of the 1994–1996 Ebola outbreaks. *Photogrammetric Engineering and Remote Sensing*, 68, 147–152.
- Walsh, P.D., Biek, R., and Real, L.A., 2005. Wave-like spread of Ebola Zaire. *PLOS Biology*, 3, 1946–1953.

- World Health Organization, 1978a. Ebola haemorrhagic fever in Sudan, 1976. Report of a WHO/International Study Team. *Bulletin of the World Health Organization*, 56, 247–270.
- World Health Organization, 1978b. Ebola haemorrhagic fever in Zaire, 1976. *Bulletin of the World Health Organization*, 56, 271–293.
- World Health Organization, 1995. Ebola haemorrhagic fever. *Weekly Epidemiological Record*, 70, 359.
- World Health Organization, 2004. Ebola haemorrhagic fever in south Sudan – update (24 May 2004). *Epidemic and Pandemic Alert and Response*. Geneva.
- World Health Organization, 2005. Marburg haemorrhagic fever: Fact Sheet (March 2005). *Media Centre*. Geneva.
- Yates, T.L., Mills, J.N., Parmenter, R.R., Ksiazek, T., Parmenter, C.A., Vande Castle, J.R., Calisher, C.H., Nichol, S.T., Abbott, K.D., Young, J.C., Morrison, M.L., Beaty, B.J., Dunnum, J.L., Baker, R.J., Salazar-Bravo, J. and Peters, C.J., 2002. The ecology and evolutionary history of an emergent disease: Hantavirus pulmonary syndrome. *BioScience*, 52, 989–998.
- Zeller, H., 2000. Lessons from the Marburg virus epidemic in Durba, Democratic Republic of the Congo (1998–2000). *Médecine Tropicale*, 60, 6–7.